

# Methodological comparison between fiber photometry and miniaturized endoscopes

1 **V.P.M. Borges\***

2 <sup>1</sup>Laboratory of Integrative Neurophysiology (INF), Center for Neurogenomics and Cognitive  
3 Research (CNCR), Vrije Universiteit Amsterdam, The Netherlands

4 **\* Correspondence:**

5 Vinicius Borges

6 mecanismoseducacao@gmail.com

7 **Keywords: one-photon calcium imaging, fiber photometry, miniscopes**

8 **Abstract**

9 Over the last decade, developments in calcium imaging have provided helpful tools for the  
10 study of brain function. This review describes recent advances in the field, especially regarding the  
11 two main techniques used to record neurophysiological activity in freely moving animals: fiber  
12 photometry and miniaturized endoscopes (miniscopes). Fiber photometry is used to investigate bulk  
13 activity changes in synchronous-firing neuronal populations while miniscopes can be used to  
14 visualize neuronal activity at the single-cell level. This review compares the implementation (e.g.  
15 technical considerations, surgeries), data acquisition, and data analysis of both techniques, providing  
16 insights into the types of research questions suitable for each method.

17 **1 Introduction – A brief history of calcium imaging**

18 To study brain function in the context of Behavioral Neuroscience, various manipulations of  
19 brain activity such as pharmacology, optogenetics, or chemogenetics have been used. These  
20 interventionistic methods of study allow scientists to make claims of function in a counterfactual  
21 manner: “activity of cell-type X in brain region Y is necessary and sufficient for behavior Z”.  
22 However, if one wants to observe patterns that emerge in the animal’s brain in a more naturalistic  
23 way, methods of direct assessment of brain activity are necessary.

24 One such method is *in vivo* recording of electrophysiological parameters, which provides  
25 unparalleled temporal accuracy and accurate estimation of spike timing of single units (Li et al.,  
26 2019). For decades, the field was predominantly attempting to unveil mechanisms of information  
27 encoding at the single-cell level, using techniques as patch-clamping in slices of brain tissue. The  
28 idea of using multicellular electrophysiology to assess simultaneous brain activity *in vivo* was met  
29 with significant skepticism: the brain was thought to be too complex to be usefully reduced to the  
30 encoding properties of only a few dozen single-units (Nicolelis, 2011). This was first proven wrong  
31 in the late 90s, in an experiment that demonstrated that the activity of 30-40 neurons accurately  
32 encoded the information of the location of a tactile stimulus (Nicolelis et al., 1998). Since then, *in*  
33 *vivo* electrophysiology has seen significant advances, culminating in inventions such as the  
34 neuropixel probe (Jun et al., 2017), which can record thousands of single units simultaneously in  
35 multiple brain regions.

36 In line with the growing interest in the investigation of neuronal population dynamics, calcium  
37 imaging technology has evolved concurrently. Initially, this method was performed with small  
38 calcium-sensitive dyes (Cobbold & Rink, 1987), and more recently with genetically encoded calcium  
39 indicators (GECIs) such as GCaMP (Nakai, Ohkura, & Imoto, 2001). The main advantage of GECIs  
40 over calcium-sensitive dyes is that they can be expressed long-term and can potentially bypass  
41 invasive loading procedures with the use of transgenic lines.

42 Calcium imaging utilizes a reporter that transforms calcium availability – which is a second-  
43 order effect of cell activity – into a fluorescent signal (Scanziani & Häusser, 2009). Therefore, this  
44 method is necessarily indirect, and it consequently has a poorer temporal resolution than  
45 electrophysiology due to limitations intrinsic to the dynamics of the calcium indicator. However,  
46 calcium imaging has a great advantage over *in vivo* electrophysiology, which is the ability to target  
47 specific neuronal-projections, cell-types, or even subcellular structures, allowing for microcircuit-  
48 level studies (Campos, 2019).

49 *In vivo* calcium imaging has commonly been performed with head-fixed animals and two-  
50 photon microscopy. Two-photon microscopy has several advantages over one-photon/widefield  
51 microscopy, including better tissue penetration, less phototoxicity due to the use of longer  
52 wavelengths, and the fact that excitation light is focused on a very narrow focal plane, resulting in a  
53 better signal-to-noise ratio (Helmchen, 2009). However, the necessity to head-fixate animals and the  
54 average price of a two-photon setup being around half-a-million dollars (Girven & Sparta, 2017) has  
55 instigated the necessity to search for cheaper 1-photon alternatives that could be used in freely  
56 moving animals. Furthermore, a comparison of the same sample under one-photon and two-photon  
57 microscopy have shown that both techniques yielded the same neurons in the image stack and with a  
58 similar pattern of signal acquisition (Glas et al., 2019), implying that one-photon can yield similar  
59 results to two-photon approaches.

60 This review will discuss two main techniques of one-photon *in vivo* calcium imaging that allow  
61 Behavioral Neuroscience studies in freely moving animals: fiber photometry and miniaturized  
62 endoscopes (miniscopes). Each technique will be examined and compared in multiple aspects,  
63 including surgeries, impact on behavior, data interpretation, and data analysis. We will describe  
64 which technique is more appropriate based upon one's research question and conclude with  
65 perspectives for the field of Behavioral Neuroscience, indicating current limitations and how they  
66 could be overcome with future technological advances.

## 67 2 GCaMP usage in calcium imaging

68 Neuronal activity is primarily an electric phenomenon which can be visualized directly using  
69 voltage indicator probes (Barnett et al., 2012), or indirectly by targeting molecules that increase in  
70 concentration as a result of cell activity, such as fluorescent biosensors for neurotransmitters (Marvin  
71 et al., 2013) or ion sensors (Arosio & Ratto, 2014). The use of voltage indicator allows for a greater  
72 temporal resolution, but their use is currently limited due to poor signal-to-noise ratio (Resendez et  
73 al., 2016). The remainder of the review will focus mainly on calcium indicators as they are the most  
74 commonly used probe for FP and miniscopes.

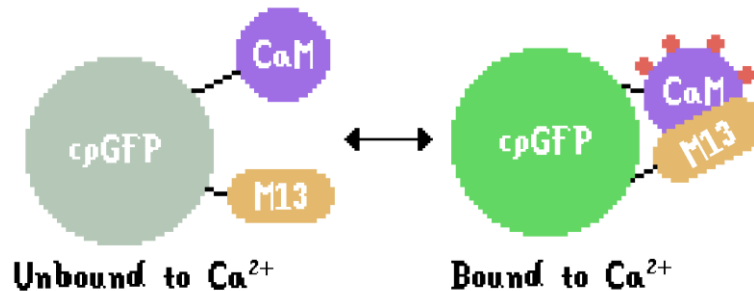
75 One of the numerous downstream consequences of neuronal activity is the increase in  
76 intracellular calcium (Ross, 1989). Calcium is important as second-messenger for many biological  
77 functions: G-protein coupled receptor activation cascades (Ma et al., 2017), neurochemicals  
78 exocytosis (Augustine, Charlton, & Smith, 1985), and synaptic plasticity (Zucker, 1999). Because  
79 calcium has a very low intracellular concentration when a neuron is inactive (0.05-0.1 mM) and a  
80 significantly higher concentration when a neuron is active (0.7-1 mM), it is a reliable target for optic

## Methodological comparison between fiber photometry and miniaturized endoscopes

81 probing, with a distinguishable signal-to-noise ratio between both states of activity (Oh, Lee, &  
82 Kaang, 2019).

83 The GCaMP protein is comprised of three portions: cpGFP (a fluorescent indicator),  
84 calmodulin (a highly sensitive calcium sensor), and M13 (a small peptide that allows a dynamic  
85 change between active and inactive states). cpGFP becomes fluorescent when excited with light in  
86 the blue color-range (around 470-490 nm). Because some energy is lost to vibration, the emitted  
87 photons from the reporter are in the green color range (around 510 nm). The difference between  
88 excitation and emission light is called Stokes Shift, and it allows the separation of excitation and  
89 emission photons with optical filters (Berezin & Achilefu, 2010).

90 The molecule of GCaMP has two conformations (**Figure 1**): unbound to  $\text{Ca}^{2+}$ , which emits less  
91 fluorescence, and bound to  $\text{Ca}^{2+}$ , which has a different protonation state (Barnett, Hughes, &  
92 Drobizhev, 2017) and results in a different protein conformation that emits significantly more  
93 fluorescence compared to the unbound conformation – for instance, a variant of GCaMP with fast  
94 kinetics (GCaMP6f) fluoresces 27 times more in a calcium-saturated state compared to a calcium-  
95 depleted state (Farhana et al., 2019). Because of the pronounced 7- to 20-fold increase in calcium  
96 availability during the active neuronal state compared to the inactive state, GCaMP fluorescence can,  
97 therefore, serve as a reliable indicator of intracellular calcium concentration, which is, in turn, an  
98 indirect measurement of neuronal activity.



99  
100 **Figure 1.** Schematic of conformations of GCaMP, unbound and bound to calcium ions.

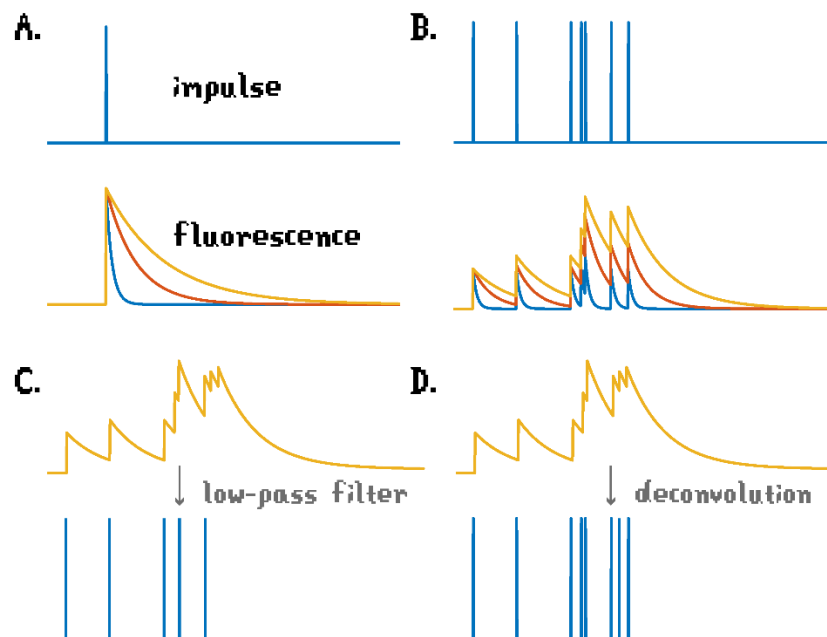
101 GCaMP is an intensimetric indicator, which means that the fluorescent signal observed  
102 depends on the concentration of GCaMP in the animal's brain. It is necessary to be cognizant of  
103 GCaMP photobleaching – i.e. the excitation light causes the degradation of GCaMP molecules –  
104 throughout a recording session. These two factors complicate the data analysis comparisons (1)  
105 between animals since different organisms will inevitably have different intracellular GCaMP levels,  
106 and (2) in the same animal because the bleaching will decrease baseline fluorescence at different  
107 timepoints of training. This is commonly addressed by using a ratio of fluorescence between active  
108 periods and baseline ( $\Delta F/F$ , see Section 8.1): although the absolute magnitude of GCaMP  
109 fluorescence might be different, the relative proportion of activity over baseline should be  
110 approximately the same, which allows comparisons of the signal within the same animal at different  
111 points in time, and also between different animals.

112 The potency of calcium indicators has significantly improved since the development of the  
113 original GCaMP probe (Nakai et al., 2001). Every iteration has roughly led to a 1.5-2x improvement  
114 of signal linearity and sensitivity (Akerboom et al., 2012; Chen et al., 2013; Tian et al., 2009). Recent  
115 innovations include the development of jGCaMP7, which has on average has 40% greater  $\Delta F/F$   
116 compared to its predecessor GCaMP6 (Dana et al., 2019), and XGCaMP, which has a four-color  
117 suite of probes which can be used for multi-color imaging (Inoue et al., 2019). Multicolor calcium  
118 indicators can be applied with photometry systems, allowing the observation of two GECIs with

119 different excitation spectra simultaneously. This allows, for instance, the combination of a red-shifted  
 120 calcium indicator combined with a green-fluorescent probe for dopamine (Beyene et al., 2018) or  
 121 simultaneous photometry measurements with optogenetics intervention in the same brain region  
 122 (Sych et al., 2019). The advantages of multicolor GCaMP suites are less applicable to miniscopes  
 123 because GRIN lenses are not appropriate to be used with red/far-red indicators (Ghosh et al., 2011).

124 There are several challenges when using this probe: GCaMP interferes with the kinetics of L-  
 125 type calcium channels (Yang et al., 2018) and there is a strong buffering of intracellular  $Ca^{2+}$  which  
 126 may lead to cytotoxicity (Resendez et al., 2016). These problems can partially be avoided by  
 127 reducing intracellular GCaMP levels, at the cost of a poorer signal to noise ratio. Therefore, an initial  
 128 dilution study is often recommended to determine optimal GCaMP expression for FP and miniscope  
 129 implementation. Furthermore, abnormalities in brain function have been reported in transgenic  
 130 GCaMP lines (Steinmetz et al., 2017). Transgenic lines can be replaced by cre-dependent lines to  
 131 bypass this problem, but that requires an additional virus injection in the target brain region.

132 In the context of Behavioral Neuroscience, GCaMP data is often synced with behavioral data,  
 133 usually by performing a low-pass filter to infer spiking activity based on the fluorescence data.  
 134 Because there are GCaMP molecules with different kinetics, the output data depends on the decay  
 135 time of the probe used (**Figure 2A**). A confounding effect of the inference of spiking activity is the  
 136 fact that the concentration of calcium in the neuron remains elevated after activity – such that a 1 ms  
 137 action potential can potentially increase GCaMP fluorescence for 1-10 s (Sabatini, 2019). This has a  
 138 consequence of reducing the correlation of fluorescence data and the true spiking, such that slower  
 139 the kinetics of GCaMP, the poorer this correlation is (**Figure 2B**). When using a slow GCaMP  
 140 variant, the utilization of a simple low-pass filter processing results in the obfuscation of fast-  
 141 consecutive spikes, which could result in false-negative findings (**Figure 2C**) (Sabatini, 2019). This  
 142 problem can be minimized by performing deconvoluting processing, i.e. using a more complex  
 143 algorithm that accounts for GCaMP kinetics and the temporal information of the spiking activity to  
 144 accurately infer cellular activity. (**Figure 2D**)



145

146 **Figure 2.** Filtering of spiking by GCaMP kinetics. (A) A single impulse generates different  
 147 fluorescence signals depending on the GCaMP type used. (B) The slower GCaMP types have

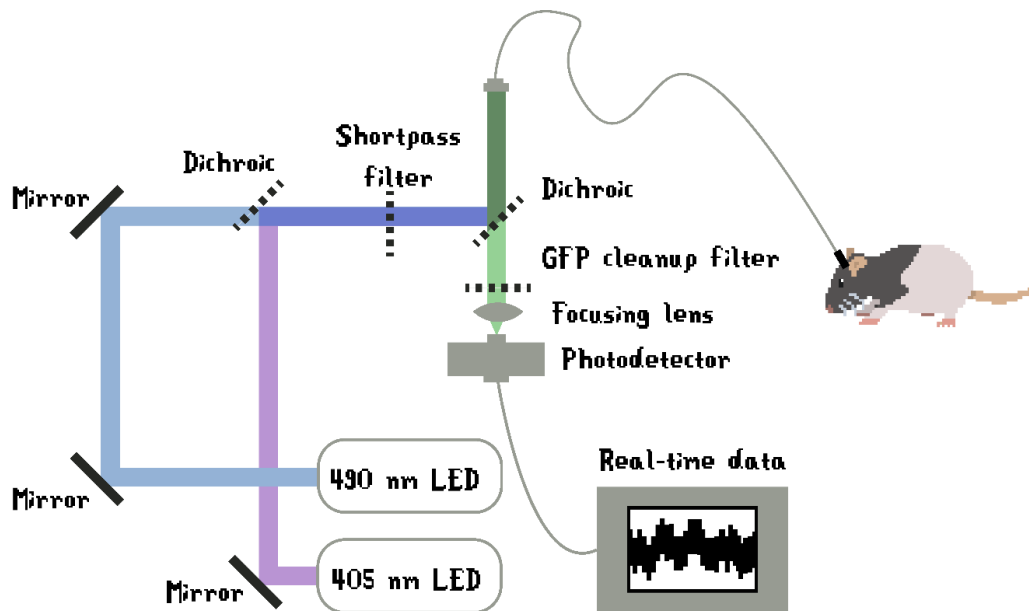
## Methodological comparison between fiber photometry and miniaturized endoscopes

148 lesser correlation coefficients between impulse and modeled fluorescent data (0.43, 0.19, and  
149 0.14 for simulated decay times of 10, 40, and 100 ms, respectively). (C) A low-pass filter can  
150 lose fast consecutive spikes because the immediate neighboring signal has a higher baseline.  
151 (D) A deconvolution algorithm uses the information from GCaMP and the proximity of  
152 fluorescent activity to achieve better results. Data recreated utilizing a MATLAB script  
153 available on [github.com/bernardosabatini/impulseCorrelations/](https://github.com/bernardosabatini/impulseCorrelations/).

154 In summary, GCaMP is one of the most commonly used and most rapidly developing GECIs in  
155 the field of neuroscience because it is one of the best optic probes in terms of signal-to-noise ratio  
156 and the fact that calcium influx is a reliable biological metric of neuronal activity. However, it is  
157 necessary to keep the limitations of GCaMP in mind: (1) it may have effects on normal physiology,  
158 especially when overexpressed in the cell. This can be minimized by an initial dilution study before  
159 the experiment; (2) it is not a real-time probe since the activity spike occurs before the influx of  
160 calcium. This, in turn, can be corrected by adding a deconvolution step in the data analysis.

### 161 3 Fiber photometry (FP)

162 FP is a calcium imaging method that uses a single patch cable, connected to an implanted fiber,  
163 to guide both excitation of the fluorescent probe and collection of the fluorescence signal (**Figure 3**).  
164 The light emitted by GCaMP in the brain of the animal can be subsequently separated with optical  
165 filters before reaching a highly sensitive detector. This analog input is converted into a digital signal:  
166 a one-dimensional trace that represents the fluorescence output of all GCaMP-tagged neurons within  
167 range of the fiber tip. Compared to traditional techniques such as electrophysiology, FP is more  
168 efficient in terms of data collection and ease of use, more stable for long-term analysis, and less  
169 expensive (Li et al., 2019).



170  
171 **Figure 3.** Simplified setup of a two-color photometry system (see Section 8.1 for the analysis  
172 pipeline). Adapted from Zalocusky et al. (2016).

173 While it lacks spatial information, FP is useful to study bulk activity of specific neuronal  
174 populations, since GCaMP can be expressed in specific cell types. Furthermore, because FP uses  
175 either a low-noise amplified photodetector or a photomultiplier tube, it has a sensitivity in the level of

176 single photons, allowing detection of low levels of activity in soma, dendrites, and axons (Dana et al.,  
177 2019). The use of a lock-in amplifier and high sensitivity detectors also allow for multiple hour-long  
178 recordings over multiple weeks with minimal signal loss due to low excitation light intensity required  
179 (Simone et al., 2018). Furthermore, it is possible to implant several fibers to assess the activity of  
180 multiple brain regions simultaneously (Kim et al., 2016) due to the relatively small size of the  
181 implant (200-400 $\mu$ m).

182 Traditional FP has a larger cone of detection (200-450  $\mu$ m) (Kupferschmidt et al., 2017;  
183 Pisanello et al., 2018) compared to the relative narrow z-resolution of the miniscope (33.35  $\mu$ m per  
184 plane of focus) (Glas et al., 2019). Recent developments with tapered fiber tips allow for light  
185 collection up to 2000  $\mu$ m depth, while their decreased surface area also reduces the amount of tissue  
186 damage (Pisano et al., 2019). Therefore, FP seems to be the most appropriate option to study the  
187 dynamics of sporadically tagged neurons, since it is unlikely that miniscopes would capture multiple  
188 cells from a sparse neuronal population within a single detection plane.

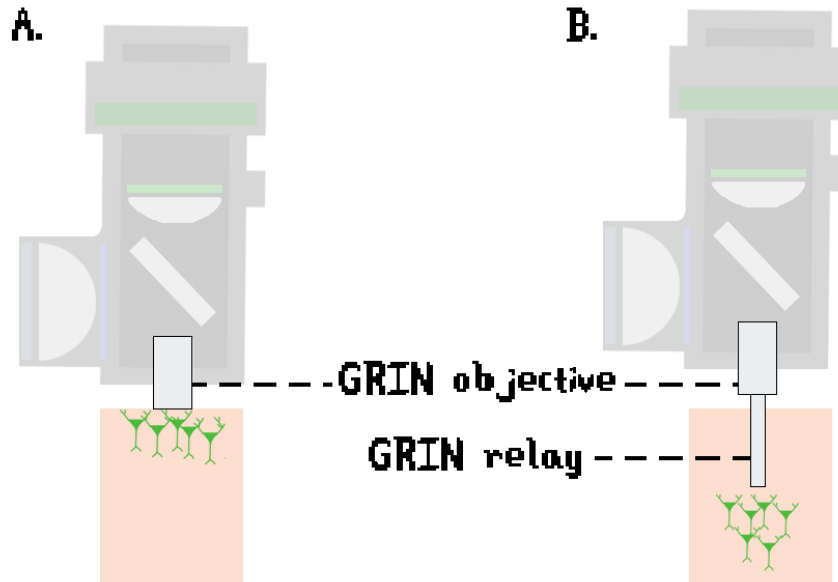
189 In summary, FP is used to assess bulk activity of neuronal populations in freely moving  
190 animals. The main limitation of the technique is the lack of spatial information, which makes it  
191 possible to use more sensitive detectors and have a great volume of acquisition, while simplifying  
192 several steps of implementation (surgery, data acquisition, and data analysis), making it a relatively  
193 straightforward technique to establish in the lab.

#### 194 **4 Miniscopes**

195 For a long time, the main limitation of one-photon calcium imaging was that brain tissue  
196 presents high levels of light scattering (Bollmann & Engert, 2009; Hamel et al., 2015), which  
197 explains why miniscopes were initially developed with two-photon technology. The original system  
198 essentially connected excitatory light from a two-photon tabletop system into a fiber that could be  
199 implanted in the animals' head, with the original implant weighing about 25 g (Helmchen et al.,  
200 2001). While other lighter two-photon miniscopes have been developed and used successfully since  
201 then, the technical challenges of optical limitations, inferior sampling rates, and movement artifacts  
202 originating from the use of long wavelengths in femtosecond pulses (Silva, 2017) have instigated the  
203 search for one-photon miniscope alternatives.

204 The problem of one-photon light scattering and consequent inability to reach more deeply  
205 than a few millimeters in the brain (Ouzounov et al., 2017) has been partially addressed by the  
206 development of GRIN lenses. GRIN lenses have a radially-varying index of refraction, which  
207 maximizes the amount of light that reaches the sensor while minimizing optical aberrations (Barretto,  
208 Messerschmidt, & Schnitzer, 2009). The miniscope contains a GRIN objective (1.8 to 2.0 mm  
209 diameter; **Figure 4A**), which is sufficient for cortical imaging (Aharoni & Hoogland, 2019). Deeper  
210 brain regions require implantation of a second GRIN relay lens (ranging from 500  $\mu$ m to 1000  $\mu$ m in  
211 diameter; **Figure 4B**).

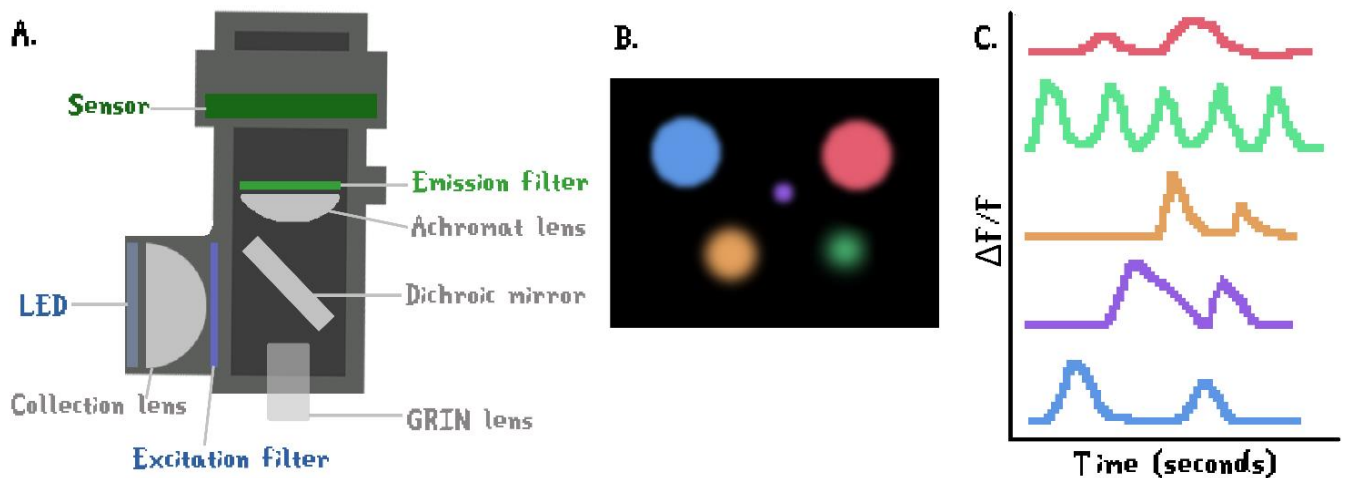
## Methodological comparison between fiber photometry and miniaturized endoscopes



212

213 **Figure 4.** Schematic of types of miniscope recording. (A) Superficial cortical recording. (B)  
214 Deep brain imaging

215 The first one-photon miniaturized microscope that allowed for single-cell resolution was  
216 developed first by the Schnitzer group at Stanford (Ghosh et al., 2011). Advances in miniaturization  
217 technology were used to replace the main components of a traditional widefield microscope with  
218 something that the animal could carry on top of its head: they replaced a lamp with a LED, a huge  
219 CCD sensor with a tiny CMOS sensor and a big objective by a small GRIN lens (**Figure 5A**). The  
220 development of miniscopes was a substantial advance for Behavioral Neuroscience: miniscope data  
221 allows researchers to visually observe the same neuronal population over multiple weeks (**Figure**  
222 **5B**) while distinguishing the contributions of single neurons to behavior (**Figure 5C**).



223

224 **Figure 5.** Schematic of miniscope structure and data visualization. (A) General components  
225 of a miniscope; (B) Neuronal populations observed with a miniscope camera; (C)  $\Delta F/F$  traces  
226 for single neurons in miniscope data (see Section 8.2 for specifics of the analysis pipeline).



227 The use of miniscopes poses technical challenges involving surgery, impact on behavior, and  
228 data analysis, which will be described in the following sections (see Sections 5, 6, and 7). Other  
229 disadvantages include that there are no waterproof miniscopes, rendering it unfeasible for behavioral  
230 paradigms such as the Morris water maze or the forced swim test (Resendez & Stuber, 2015).  
231 Furthermore, modern miniscopes systems have limited acquisition frame rates, precluding the use of  
232 temporally precise voltage-sensors (Hamel et al., 2015).

233 In summary, miniscopes can provide significantly more information than fiber photometry:  
234 rather than collapsing all information into a single dimension, miniscope data preserves the spatial  
235 organization of the neurons in the field-of-view. However, while providing single-cell resolution, the  
236 system is more technically challenging to implement and more difficult to analyze.

## 237 **5 Surgery**

238 FP and miniscope both require stereotactic surgery to ensure accurate implant placement.  
239 Surgical procedures are similar: (1) Virus injection to express GCaMP (when not using a transgenic  
240 line); (2) implantation of fiber/GRIN lens; (3) headcap placement; (4) for miniscope, baseplate  
241 placement to allow secure connection of the device onto the headcap. When using a viral expression  
242 of GCaMP, both techniques benefit from a preliminary dilution study, in which multiple  
243 concentrations of the virus are tested. The goal is to have optimal GCaMP expression, which is  
244 visually expressed throughout the cytosol, but not the nucleus (Resendez et al., 2016), since  
245 overexpression will lead to excessive buffering of calcium ions and eventual cell death (Grienberger  
246 & Konnerth, 2012).

247 The placement of implants requires similar steps for both techniques: making a craniotomy,  
248 dura removal, and placement of the fiber or GRIN lens. However, a few complications may arise in  
249 the miniscope surgery due to the greater size of the implant. Large GRIN lenses also increase  
250 intracranial pressure, potentially leading to shifts in virus diffusion and subsequent mistargeted  
251 GCaMP expression. To minimize this issue, one could inject a 15% d-mannitol to reduce intracranial  
252 pressure before drilling the holes in the skull (de Groot et al., 2020).

253 GRIN relay lenses (500  $\mu\text{m}$  – 1000  $\mu\text{m}$ ) are significantly more damaging to the brain than a  
254 fiber implant (200  $\mu\text{m}$  – 400  $\mu\text{m}$ ) because a two-fold increase in diameter will result in a four-fold  
255 increase in volume (and thus four times more damaged or displaced cells). An important  
256 consideration is that the relative impact of the implant diminishes with the size of the animal model.  
257 For example, an implant of the same size will induce a proportionally higher volume of damage in a  
258 mouse brain, which weighs between 0.4-0.5 g, compared to a rat brain, which weighs around 2 g  
259 (Bolon & Butt, 2011).

260 The amount of tissue damage is also dependent on the brain region of interest: the more ventral  
261 in the brain, the larger the GRIN relay lens needs to be to assure proper signal acquisition, and  
262 consequently more tissue needs to be removed for the implant. This may preclude one from using the  
263 miniscope in ventral brain regions – such as the OFC – since a significant volume of dorsal tissue  
264 would need to be removed, which could lead to confounding behavioral effects.

265 To summarize, even though the surgery steps are similar for FP and miniscopes, the difference  
266 in implant size needs to be taken into account in the experimental design, both for which animal  
267 model to use and for which brain region one is trying to collect data from.



### 268 **6 Impact on behavior**

269 FP and miniscope systems both require headcaps and the attachment of cables. Important  
270 considerations for behavior are: 1) Secondary consequences of individual housing; 2) Induction of  
271 stress related to the attachment of the animal to the device and; 3) Limitations of movement as a  
272 consequence of the size and weight distribution of the apparatus.

273 Because the animals have a reasonably fragile implement permanently attached to the top of  
274 their heads, most protocols for FP and miniscopes advise that researchers put their animals in  
275 individual housing after surgery. Studies have shown that single housing, even in an enriched  
276 environment, leads to significant changes in stress levels (Krohn et al., 2006), therefore leading to an  
277 unknown source of unsystematic bias in behavioral studies (Manouze et al., 2019).

278 The connection between headcap and device is different between the two techniques: attaching  
279 a cable to the animals headcap for FP is a matter of sliding a cable into a ferrule and can be  
280 performed by a single person. On the other hand, the miniscope needs to be fixed onto the baseplate  
281 with two screws, which can be more stressful for the animal. Some protocols recommend brief  
282 anesthesia every time the animal needs to be attached or detached from the miniscope (Yang et al.,  
283 2015), which is problematic because repeated anesthesia has significant side-effects on the animal's  
284 health (Hohlbaum et al., 2017) and a long-lasting effect on brain activity (Wu et al., 2019). An  
285 alternative is to perform extensive habituation, which could be aided by work with custom head-fixed  
286 setups in which the rodent can run on a treadmill (de Groot et al., 2020) while the scope is being  
287 attached to reduce the stress of the animal. The latter setup requires more extensive habituation of the  
288 animal to the setup, while also being more expensive and laborious because it requires two  
289 researchers – one who holds the ring in place and the other who secures the miniscope with screws.

290 The miniscope headcap covers a larger skull surface area and volume compared to the fiber  
291 photometry headcap. The ring-shaped structure that supports the baseplate for the miniscope usually  
292 weighs a few grams (Resendez et al., 2016), which is often unaccounted in the miniscope weight. In  
293 terms of direct influence on behavior, it is important to consider the weight of the devices – with the  
294 photometry fiber is lighter than the miniscope device – but also how the weight is distributed:  
295 although miniscopes have become as light as 1.6 grams (de Groot et al., 2020), they still have a high  
296 center of gravity compared to fiber photometry. This creates a stronger torque and potentially  
297 interferes more intensely with the animal's vestibular system, especially for mice compared to rats  
298 due to their smaller body size.

299 To summarize, even though the size of a miniscope has been reduced because of rapid open-  
300 source development, it is still a bigger device with a higher center of gravity and a greater impact on  
301 behavior compared to FP.

### 302 **7 Data acquisition**

303 Both FP and miniscope systems have commercial and open-source hardware and software for  
304 data acquisition, each with advantages and disadvantages. The main challenge in data acquisition for  
305 calcium data revolves around maintaining the same field-of-view over multiple days of recording.

306 Regarding hardware cost, there are two big manufacturers of photometry setups which are  
307 widely adopted: Doric and Tucker-Davis Technologies. These off-the-shelf photometry systems may  
308 cost around 10,000-20,000 dollars, but recent open-source alternatives are currently available for  
309 optical components (Simone et al., 2018), the acquisition interface and GUI (Akam & Walton, 2019;

310 Owen & Kreitzer, 2019), resulting in a photometry system which costs about one-tenth of the price of  
311 traditional systems (Owen & Kreitzer, 2019).

312 On the other hand, the miniscope community is intensely driven by open source contributions,  
313 which rapidly accelerates the development of new technology and design. Since the original 1P  
314 miniscope (Ghosh et al., 2011), several one-photon miniscopes systems were developed and became  
315 available to the scientific community: the NiNscope has a built-in optogenetic driver and  
316 accelerometer, the FinchScope is optimized for birds as a model species and it has a microphone to  
317 correlate vocalization with neuronal activity, the Inscopix nVista V4 has a sophisticated focusing  
318 system, such that different z-planes can be interweaved acquired very rapidly (full review available  
319 from Aharoni & Hoogland, 2019). Although off-the-shelf proprietary systems such as the Inscopix  
320 scope are priced at around 70,000 dollars, open-source alternatives such as the UCLA miniscope  
321 allow the construction of a system for about 1,500 dollars.

322 It is critical to record the same neuronal population over multiple days to be able to accurately  
323 interpret the output. Because miniscopes have cellular visualization, one can adjust the focus ring  
324 from to maintain the same plane of acquisition. This is impossible for FP because it lacks cellular  
325 resolution. Moreover, the cable can occasionally slip from the animal's head during FP recordings  
326 with detachable cables, resulting in the recording of a smaller subset of the tagged population over  
327 the session. This can be partially remedied by using a low-loss coupling interconnect (such as the  
328 ADAL3 from ThorLabs) between the implanted fiber and cable.

329 During the recording session, for both FP and miniscopes, it is necessary to always have an  
330 experimenter attentive to changes in the fluorescence signal and to take note of any anomalies that  
331 might occur (e.g. animals damaging the cable). Failure to do so might lead to improperly annotated  
332 data and could lead to incorrect conclusions, e.g. decrease in fluorescence being incorrectly ascribed  
333 to changes in behavior. To minimize the chances of cable damage, a rotary joint can be used to  
334 minimize torque forces on the cable. Another promising technology to eliminate the issue of cable  
335 damage is the development of wireless photometry (Khiarak et al., 2018) or wireless miniscope  
336 systems (Barbera et al., 2019).

337 To summarize, both FP and miniscope require thorough consideration in the steps of data  
338 acquisition to ensure that the same population is recorded over multiple days. This problem more  
339 easily dealt with in miniscopes, by manual or electronically focusing, but it can also be minimized  
340 with hardware changes in FP systems, mainly low-loss connectors.

## 341 **8 Data analysis**

342 FP and miniscope have significantly different analysis pipelines, owing to the greater  
343 complexity of miniscope data compared to FP data. In order to properly interpret the results, it is  
344 important to understand the core ideas of each analysis pipeline as well as limitations intrinsic to each  
345 method and associated behavioral task.

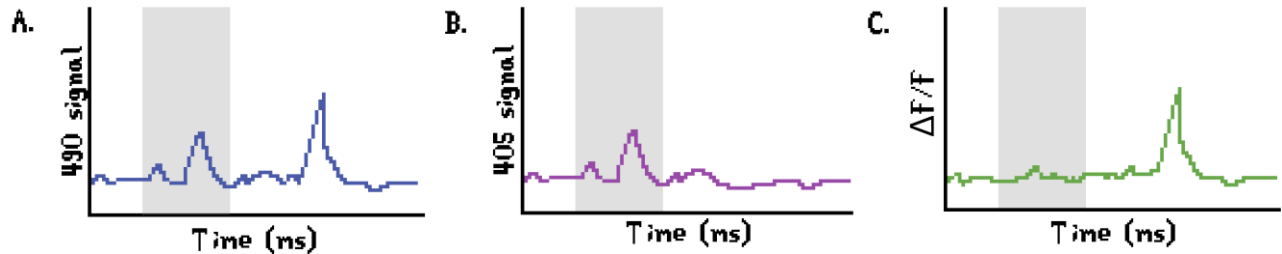
### 346 **8.1 Photometry data analysis**

347 In terms of data complexity, FP data constitutes a simple database that stores incoming  
348 fluorescence in a one-dimensional time series (often 100-200 MB/hour). Photometry data analysis  
349 consists of two main steps: motion correction and correlation with behavior. Movement artifacts can  
350 be resolved in two ways. One option is to use time-correlated single-photon counting, which uses  
351 rapid oscillation of the excitation light and uses post-hoc analysis to isolate the fluorescence signal

## Methodological comparison between fiber photometry and miniaturized endoscopes

352 (Gunaydin et al., 2014). Another option is to make use of two excitation lights, a blue light to excite  
353 GCaMP and a purple light, which is GCaMP-insensitive and serves as a control channel (Zalocusky  
354 et al., 2016, **Figure 6**). With this system, the  $\Delta F/F$  is calculated with a straightforward formula:

$$355 \quad \frac{\Delta F}{F} = \frac{\text{Signal}_{490nm} - \text{Signal}_{405nm}}{\text{Signal}_{405nm}}$$



356  
357 **Figure 6.** Visualization of  $\Delta F/F$  calculation for fiber photometry. Motion artifacts can be  
358 observed when the blue and purple signals follow the same pattern (grey segment). By  
359 adjusting the GCaMP-dependent signal (A) with the GCaMP-independent signal (B), it is  
360 ensured that the output (C) is representative of actual GCaMP activity.

361 The  $\Delta F/F$  signal is then usually aligned with behavioral performance, such as lever presses,  
362 nose pokes, and food magazine entries. The experimenter often chooses a time window which is  
363 representative of the brain function they would like to assess, for instance, during the preparatory  
364 attention phase in a choice paradigm to indicate impulse control or before a lever press to assess  
365 motor planning. Many parameters can be used to compare  $\Delta F/F$  traces, ranging from area under the  
366 curve and maximum peak amplitude calculations, to inferences of spikes from deviations of baseline  
367 activity.

368 Although the data acquired from the photometry setup is relatively simple, the interpretation  
369 can still be challenging. Even though movement artifacts can be corrected with a  $\Delta F/F$  calculation,  
370 there is still a general effect of movement which is difficult to account for, since the execution of  
371 movement results in a brain-wide increase of activity (Musall et al., 2019) even in sensory areas  
372 (Parker et al., 2020). Because the animal is freely moving, exact behavior and movement will vary on  
373 a trial-to-trial basis, which means that even when selecting the same time windows around task  
374 events, one might find differences in fluorescence signal – not because there is a change in cognitive  
375 function, but because there is a difference in how much the animal is moving at these time points. In  
376 the context of mPFC studies, this is known as the ‘Euston-Cowen-McNaughton Hassle’ (Powell &  
377 Redish, 2016), the observation that differences in brain activity can be explained by differences in  
378 movement at different trial periods. It is worth noting that this effect of movement in brain activity is  
379 also present in miniscope data, although the spatial information allows for the general separation of  
380 ‘movement-related’ and ‘movement-unrelated’ neurons (da Silva, 2018), which is not possible for FP  
381 data.

## 382 8.2 Miniscope data analysis

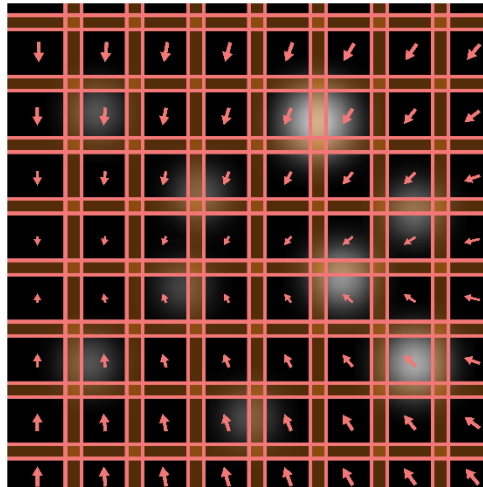
383 Compared to the one-dimensional time series data collected from fiber photometry, miniscope  
384 data is multidimensional and present several challenges. First, miniscope data is acquired in a video  
385 format and data acquisition can come up to 100 GB/hour (Pnevmatikakis, 2019), which means that

386 miniscope data analysis requires significantly better hardware and IT infrastructure for storage and  
 387 retrieval of potentially multiple terabytes of data for each experiment. Second, the steps of  
 388 registration, source separation, and deconvolution need to be high-throughput due to the large data  
 389 size.

### 390 8.2.1 Registration

391 Because the brain is a soft organ, it moves and deforms as the animal is moving, and neurons in  
 392 the field-of-view move in a non-rigid fashion over time, i.e. some neurons might move in different  
 393 directions while others stay in place. Therefore, a straightforward rigid movement correction, i.e.  
 394 moving the entire frame by  $x$  pixels, is not adequate for miniscope datasets, because they result in  
 395 neurons being in different locations in the field-of-view over time. A solution is a non-rigid form of  
 396 registration, which takes into account the brain deformation, for instance, by modeling topological  
 397 features of elastic bodies and inferring the underlying motion (Ahmad & Khan, 2015) or utilizing  
 398 probabilistic methods to track the same neurons in different positions across time (Sheintuch et al.,  
 399 2017). These non-rigid solutions require significantly more computational power compared to rigid  
 400 registration methods.

401 The most commonly used method for image registration of miniscope data is the NoRMCorre  
 402 algorithm (Pnevmatikakis & Giovannucci, 2017), which uses rigid registration to arrive at non-rigid  
 403 results. To accomplish that, the algorithm subdivides the video input into a grid of overlapping  
 404 sections (**Figure 7**). It then applies a rigid motion correction to every single section of the video (e.g.  
 405 move the entire section upward  $x$  pixels). The smaller the sections, the better the approximation to a  
 406 proper non-linear registration it will be. The entire frame is then reconstructed by stitching the  
 407 overlapping portions of these segments. Instead of repeating the process *de novo* for every frame, a  
 408 template frame is stored, and every subsequent frame is calculated in reference to the template to  
 409 optimize processing time.



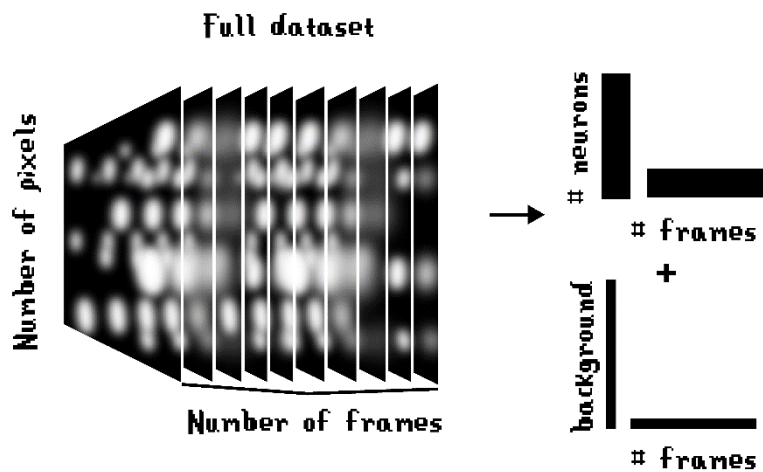
410

411 **Figure 7.** Visualization of the NoRMCorre algorithm strategy of registration. The arrows  
 412 represent how much each subsection moves in one direction, while the orange shaded area represents  
 413 the overlap between each subsection, which is used to reconstruct the whole frame afterward.

414 **8.2.2 Source separation**

415 With a stabilized video, the next challenge is to separate every neuron in the frame. This is  
 416 computationally challenging because of the size of video files. It is also worth noting that one-photon  
 417 imaging captures a lot of neuronal sources outside the plane of focus, which must be accounted for in  
 418 the analysis. Furthermore, background noise essentially changes every frame in one-photon data.

419 The most widely used algorithm for source separation of one-photon miniscope data is CNMF-  
 420 E (Zhou et al., 2018). This algorithm does not store all the information from every pixel in every  
 421 frame of the video. Instead, it only captures the information from the fluorescence sources in the  
 422 field-of-view and an average of the background fluorescence, allowing for a great compression of  
 423 data size (**Figure 8**). Once the video information is unveiled into separate components, it is possible  
 424 to use a memory infrastructure that allows parallel processing, making use of multiple CPU cores to  
 425 optimize processing time.



426

427 **Figure 8.** Visualization of the CNMF-E method of data compression.

428 A problem that needs to be addressed by the source separation algorithm is the fact that there  
 429 are overlapping neurons in three-dimensional space that occupy the same pixels in the x-y field of  
 430 view. This is usually not taken into account when source separation is performed with simpler  
 431 methods such as manual region-of-interest annotation or PCA/ICA methods (Zhang et al., 2019).  
 432 CNMF-E can separate neurons with a great overlap in the field of view, distinguishing the different  
 433 sources by their different periods of activity.

434 A quality check for the soma shape is required after the putative neurons have been identified  
 435 and separated. This task can be performed manually or with the assistance of machine learning  
 436 methods. The use of unbiased machine learning methods is important because even among expert  
 437 annotators there can be a disagreement level of 20% (Pnevmatikakis, 2019).

438 **8.2.3 Deconvolution**

439 The resulting fluorescence signal depends on the sensitivity and kinetics of the GCaMP isoform  
 440 used. Therefore, after source separation, the fluorescence signal needs to be deconvolved into spike  
 441 activity. Importantly, prior to deconvolution, the data needs to be detrended to remove the influences  
 442 of photobleaching throughout the recording. A common deconvolution method is the OASIS  
 443 algorithm (Friedrich, Zhou, & Paninski, 2017), which has been benchmarked as superior against nine  
 444 other deconvolution methods (Berens et al., 2017).

445 **8.2.4 Comparison of open-source packages**

446 To facilitate the workflow of the several steps required for miniscope data analysis, several  
 447 open-source packages compile the required tools for registration, source separation, and  
 448 deconvolution, including CalmAn (Giovannucci et al., 2019) EZCalcium (Cantu et al., 2020),  
 449 MiniscopeAnalysis and its subsequent implementation of PIMP (Etter, Manseau, & Williams,  
 450 2020), MINIPIPE (J. Lu et al., 2018) and CAVE (Tegtmeier et al., 2018) (**Table 1**).

451 **Table 1.** Overview of commonly used miniscope analysis packages.

Analysis Package (Institute)	Short description	Registration Method	Source Separation Method	Deconvolution Method	References
CalmAn (Simons Foundation)	Well-documented pipeline, updated often, can be used for 1- or 2-photon data. Python based.	NoRMCorre	CNMF or CNMF-E	OASIS	Giovanucci et al. (2019)
EZCalcium (UCLA)	Adoption of CalmAn in a easy-to-use graphical user interface. Currently only available for two-photon data.	NoRMCorre	ROI detection	OASIS	Cantu et al. (2020)
MiniscopeAnalysis (UCLA/McGill University)	Depracted pipeline. MATLAB based.	NoRMCorre	CNMF-E	OASIS	Etter et al. (2020) <a href="https://github.com/etterguillaume/MiniscopeAnalysis">github.com/etterguillaume/MiniscopeAnalysis</a>
PIMP (UCLA/McGill University)	Updated version of MiniscopeAnalysis, integrated in Google Colaboratory (virtual Python environment).	NoRMCorre	CNMF-E	OASIS	<a href="https://github.com/etterguillaume/PIMP">github.com/etterguillaume/PIMP</a>
MINIPIPE (Duke University)	Pipeline optimized for 1-photon data. Utilizes a neural enhancing model to decrease background noise. MATLAB based.	Hierarchical KLT-Demons-based	Gaussian mixture model + recurrent neural networks + CNMF	Bayesian model inversion	Lu et al. (2018)
CAVE (Magdeburg University)	Allows for easy analysis of calcium data in conjunction with behavioral data in a easy-to-use graphical user interface.	Lucas-Kanade registration	PCA/ICA	OASIS	Tegtmeier et al. (2018)

452

453 To summarize, FP and miniscope differ enormously in their data analysis pipelines. FP data is  
 454 significantly simpler and allows for more straightforward analysis steps, whereas the spatial  
 455 information of miniscope data poses several technical challenges that need to be tackled with more  
 456 sophisticated algorithms. Data interpretation needs to be contextualized in terms of the behavioral  
 457 task the animals are performing and how well the experimental design controls for the effects of  
 458 movement in brain activity.

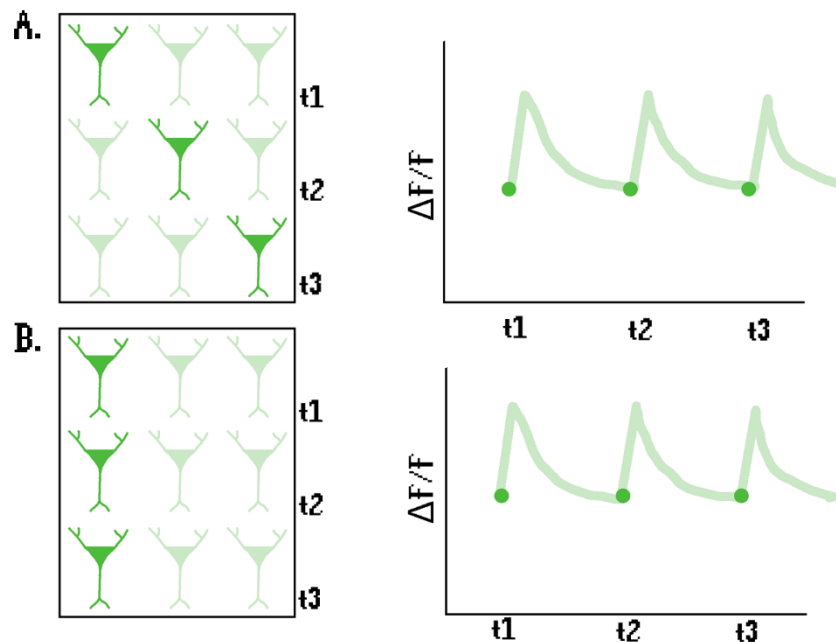
459 **9 Challenges in data interpretation**

460 The miniscope has one great advantage over photometry systems: cellular resolution. However,  
 461 this considerable advantage comes with several complications: the necessity of a larger implant in the  
 462 brain to gather sufficient light, a bigger device that interferes more intensely with the vestibular  
 463 system of the animal, and many technical challenges in data acquisition and data analysis. In this  
 464 context, there is a crucial question that needs to be addressed: Why is cellular resolution worth these  
 465 many disadvantages in the first place?

466 Consider a hypothetical scenario with a total population of three neurons. In the first scenario,  
 467 each neuron fires once, one after the other (**Figure 9A**), whereas in the second scenario, the same  
 468 neuron fires three times (**Figure 9B**). While this would be easily distinguishable with a miniscope, it

## Methodological comparison between fiber photometry and miniaturized endoscopes

469 would yield the same signal in photometry data – even though the biological meaning of each  
470 situation is radically different.



471  
472 **Figure 10.** Illustration of how the lack of spatial resolution of FP may lead to confounding  
473 effects. In a population of 3 neurons, (A) each neuron firing once and (B) the same neuron  
474 firing three times lead to the same  $\Delta F/F$  signal.

475 This example illustrates the main limitation of FP: it collapses all spatial information into a  
476 single dimension, so there is no way to differentiate the activity of different subsets of a neuronal  
477 population at different time points. For instance, miniscope studies have shown that different mPFC  
478 ensembles are active during distinct social behavior tests (Liang et al., 2018). It is conceivable that  
479 similarly sized neuronal ensembles would yield similar patterns of activity in FP data, possibly  
480 leading to erroneous interpretations of the results.

481 However, photometry data can be informative to characterize synchronous activity of a  
482 genetically separable population in a well-defined behavioral paradigm. When these conditions are  
483 met, FP has been shown to yield informative links between brain activity and behavior: examples  
484 include 1) understanding how the activity of CRH neurons in the paraventricular nucleus influence  
485 escape behavior (Daviu et al., 2020); 2) explaining the differences in activity between GABAergic  
486 and serotonergic neurons in the dorsal raphe nucleus that promote or inhibit movement in terms of  
487 threat potential (Seo et al., 2019); 3) unveiling the dynamics of hypothalamic neuronal subtypes that  
488 drive feeding behavior (Chen et al., 2015).

489 In contrast, miniscope data is multidimensional, allowing for studies where ensemble activity  
490 can be observed over time. The spatial information of neurons is important for experimental  
491 questions regarding asynchronous populations, when there is no clear genetic marker that separates  
492 different populations and when the behavior is more naturalistic and has more degrees of freedom.  
493 Examples include 1) unveiling the activity of heterogeneous ensembles of the habenula during escape  
494 behavior (Lecca et al., 2020), 2) assessing the complex dynamics hippocampal cell firing in epileptic  
495 mice (Shuman et al., 2020) and 3) understanding the relationship of how changes in the maturation of  
496 hippocampal ensembles to the consolidation of a fear memory (Kitamura et al., 2017).



497 To summarize, no technique is necessarily better for any given behavioral task – illustrated by  
498 fleeing behavior studies with FP or miniscope (Daviu et al., 2020; Lecca et al., 2020) – or brain  
499 region – illustrated by the fact that the dorsal medial striatum has been studied with both techniques  
500 (Barbera et al., 2016; Kupferschmidt et al., 2017). In general, photometry is appropriate for  
501 genetically separable and synchronous neuronal populations while the miniscope can be used for  
502 more nuanced questions, allowing the study of genetically inseparable and asynchronous ensembles.

## 503 **10 Future of calcium imaging research**

504 While it is important to consider the limitations of FP and miniscopes to properly interpret the  
505 data from these Behavioral Neuroscience studies, it is worth to scan the horizon for future  
506 developments in the field that could overcome some of the current shortcomings.

### 507 **10.1 Better optic probes**

508 As previously described (See Section 2), GCaMP is an indirect indicator of neuronal activity  
509 which may lead to confounding results when syncing fluorescence data to behavior, especially for  
510 molecules with slower kinetics (Sabatini, 2019). An alternative to calcium probes is the use of  
511 voltage indicators, which have a better temporal resolution (Resendez et al., 2016), while also  
512 avoiding problems with buffering of intracellular calcium. They have seen limited use in  
513 neuroscientific research due to a poor signal to noise ratio, but the development of brighter voltage  
514 indicators could answer a range of new biological questions (Song, Barnes & Knöpfel., 2017).  
515 Currently, FP is more appropriate for indicators with a poor signal-to-noise ratio (L. Li et al., 2017)  
516 because of its higher sensitivity of detection compared to the miniscope sensor.

517 A future alternative to the use of GCaMP could be the utilization of bioluminescent molecules  
518 as a calcium indicator (e.g. luciferase bound with calmodulin). Because these molecules do not  
519 require excitation light, confounding problems of phototoxicity are avoided, while also reducing the  
520 number of parts in a miniscope – without an excitation light, a UCLA miniscope would be 22%  
521 lighter and 58% less expensive (Celinskis et al., 2020).

### 522 **10.2 Engram-specific tagging**

523 Expressing a calcium indicator in a specific subset of neurons may give insight into whether  
524 certain projections or cell-types are active during a behavioral task. However, this tagging strategy  
525 also includes neurons unrelated to the behavior being studied (Josselyn & Tonegawa, 2020). This can  
526 confound interpretation since no systematic analysis can be done post-hoc to assess which neurons  
527 were related to the task. These confounding factors are even more problematic when analyzing  
528 associative cortices such as the mPFC, in which any given neuron may have motoric, limbic, or  
529 sensory inputs (Heidbreder & Groenewegen, 2003). An interesting technique to reduce this problem  
530 is the use of viral-based TRAP (targeted recombination in active populations) to express GCaMP  
531 only in the neurons which were naturally active during the task (Matos et al., 2019). Especially for  
532 miniscope studies, the utilization of Fos-Cre-GCaMP systems (Ivashkina et al., 2019) to assess long-  
533 term changes only in neurons that are related to a task holds a lot of promise for specifically  
534 associating shifts in neuronal activity to changes in behavior.

### 535 **10.3 Multiple-photon miniscopes**

536 Despite substantial technical challenges of two-photon miniscopes, recent models have allowed  
537 solutions for high-temporal resolution and low motion-artifacts in a light-weight, 2 g apparatus,

## Methodological comparison between fiber photometry and miniaturized endoscopes

538 allowing visualization of soma, dendrites, and axons (Zong et al., 2017). In addition, 3-photon  
539 microscopy (which uses wavelengths in the order of 1300 nm) allows the visualization of neurons in  
540 the hippocampus 1 mm below the cortical surface (Ouzounov et al., 2017). While the development of  
541 multiple-photon microscopy is currently hampered by technical challenges and expensive setups, the  
542 technology of using increasingly longer wavelengths holds promise in terms of tissue penetrance and  
543 could potentially allow the study of subcortical regions without the necessity of a GRIN lens implant.

### 544 **10.4 Simultaneous calcium imaging and video analysis**

545 Advances in Behavioral Neuroscience will include the association between neuronal activity  
546 and granular annotation of the animal's behavior from video data analysis. While proprietary  
547 software has offered some integration support (e.g. Bonsai and the UCLA miniscope) (Lopes et al.,  
548 2015), rapid advances of open-source programs like DeepLabCut (Mathis et al., 2018) will likely be  
549 commonplace in a few years. Video analysis software allows researchers to separate of movement-  
550 related neuronal activity related to cognitive effects of the task, which allow for a more accurate  
551 interpretation of

### 552 **10.5 Reduction of human interference**

553 An important consideration for Behavioral Neuroscience is the fact that stress affects brain  
554 function (Datta & Arnsten, 2019). Therefore, differences in animal handling between different labs  
555 are an important confounding factor and an important part of the current 'replicability crisis'  
556 (Lonsdorf et al., 2017). One solution is the wide adoption of rigorous and detailed protocols for  
557 animal handling, allowing for better comparisons of results and effect sizes across different labs. A  
558 technological solution is the removal of human-animal interactions altogether, aided by the  
559 development of wireless miniscopes (Barbera et al., 2019) or wireless photometry systems (Lu et al.,  
560 2018), especially if these wireless systems could be protected enough such that single-housing was  
561 no longer necessary. Another technological advance that will aid in this direction is the development  
562 of home cage systems integrated with behavioral paradigms (Bruinsma et al., 2019), notably when  
563 these technologies could be combined with an automatic weighing of the animal (Noorshams, Boyd,  
564 & Murphy, 2017). This combination of technologies would provide a significant reduction in  
565 unsystematic bias between studies, while simultaneously reducing the workload of researchers.

## 566 **11 Conclusion**

567 To conclude, both FP and miniscopes are important techniques for the advance of  
568 understanding population dynamics in freely moving animals and future technological advances hold  
569 great promise of improvement. The level of analysis at a population level is crucial for advancing the  
570 understanding of the brain because complex information is not stored in a single neuron, but rather at  
571 a sparse population level in the nervous system (Doetsch, 2000). However, it is important to keep in  
572 mind that these methods allow the observation of activity of a few hundred cells, which is only a  
573 minuscule percentage of the mouse or rat brain – which have around 70 and 200 million neurons  
574 respectively (Herculano-Houzel, Mota & Lent, 2006). The tagged neurons will also invariably  
575 contain neurons unrelated to the execution of the behavioral task (Gonzalez et al., 2019) and often  
576 contain movement-related increases in brain activity (Musall et al., 2019), leading to confounding  
577 effects on the data. Therefore, the interpretation of results acquired with these methods needs to be  
578 grounded in a solid understanding of the trade-offs and limitations of each technique.

579 **12 Conflict of Interest**

580 *The authors declare that the research was conducted in the absence of any commercial or financial*  
581 *relationships that could be construed as a potential conflict of interest.*

582 **13 Author Contributions**

583 VB wrote the manuscript with input from the other authors.

584 **14 Funding**

585 This study was funded by the Netherlands Organization for Scientific Research (NWO;  
586 917.76.360, 912.06.148; one VICI grant), ERC StG “BrainSignals,” the Dutch Fund for Economic  
587 Structure Reinforcement (FES, 0908 “NeuroBasic PharmaPhenomics project”), EU 7th Framework  
588 Programme (HEALTH-F2-2009-242167 “SynSys” and agreement no. 604102 “Human Brain  
589 Project”).

590 **15 Acknowledgments**

591 VB personally thanks the institutions that funded his studies: Vrije Universiteit (Vrije  
592 Universiteit Fellowship Programme – VUFP and Holland Scholarship Program – HSP), Nuffic Neso  
593 (Orange Tulip Scholarship), Schuurman Schimmel and Groesbeek-Assenbroek (grants for living  
594 expenses).

595 **16 References**

- 596 Aharoni, D., & Hoogland, T. M. (2019, January 29). Circuit investigations with open-source  
597 miniaturized microscopes: Past, present and future. *Frontiers in Cellular Neuroscience*.  
598 Frontiers Media S.A. <https://doi.org/10.3389/fncel.2019.00141>
- 599 Ahmad, S., & Khan, M. F. (2015). Topology preserving non-rigid image registration using time-  
600 varying elasticity model for MRI brain volumes. *Computers in Biology and Medicine*, 67, 21–  
601 28. <https://doi.org/10.1016/j.compbiomed.2015.09.022>
- 602 Akam, T., & Walton, M. E. (2019). pyPhotometry: Open source Python based hardware and software  
603 for fiber photometry data acquisition. *Scientific Reports*, 9(1). <https://doi.org/10.1038/s41598-019-39724-y>
- 605 Akerboom, J., Chen, T. W., Wardill, T. J., Tian, L., Marvin, J. S., Mutlu, S., ... Looger, L. L. (2012).  
606 Optimization of a GCaMP calcium indicator for neural activity imaging. *Journal of*  
607 *Neuroscience*, 32(40), 13819–13840. <https://doi.org/10.1523/JNEUROSCI.2601-12.2012>
- 608 Arosio, D., & Ratto, G. M. (2014). Twenty years of fluorescence imaging of intracellular chloride.  
609 *Frontiers in Cellular Neuroscience*, 8(1), 258. <https://doi.org/10.3389/fncel.2014.00258>
- 610 Augustine, G. J., Charlton, M. P., & Smith, S. J. (1985). Calcium entry and transmitter release at  
611 voltage-clamped nerve terminals of squid. *J. Physiol*, 361, 163–181. Retrieved from  
612 <https://www.ncbi.nlm.nih.gov/pmc/articles/PMC1193058/pdf/jphysiol00565-0174.pdf>
- 613 Barbera, G., Liang, B., Zhang, L., Gerfen, C. R., Culurciello, E., Chen, R., ... Lin, D. T. (2016).  
614 Spatially Compact Neural Clusters in the Dorsal Striatum Encode Locomotion Relevant

## Methodological comparison between fiber photometry and miniaturized endoscopes

- 615 Information. *Neuron*, 92(1), 202–213. <https://doi.org/10.1016/j.neuron.2016.08.037>
- 616 Barbera, G., Liang, B., Zhang, L., Li, Y., & Lin, D. T. (2019). A wireless miniScope for deep brain  
617 imaging in freely moving mice. *Journal of Neuroscience Methods*, 323(March), 56–60.  
618 <https://doi.org/10.1016/j.jneumeth.2019.05.008>
- 619 Barnett, L. M., Hughes, T. E., & Drobizhev, M. (2017). Deciphering the molecular mechanism  
620 responsible for GCaMP6m's Ca<sup>2+</sup>-dependent change in fluorescence. *PLOS ONE*, 12(2),  
621 e0170934. <https://doi.org/10.1371/journal.pone.0170934>
- 622 Barnett, L., Platisa, J., Popovic, M., Pieribone, V. A., & Hughes, T. (2012). A Fluorescent,  
623 Genetically-Encoded Voltage Probe Capable of Resolving Action Potentials. *PLoS ONE*, 7(9).  
624 <https://doi.org/10.1371/journal.pone.0043454>
- 625 Barretto, R. P. J., Messerschmidt, B., & Schnitzer, M. J. (2009). In vivo fluorescence imaging with  
626 high-resolution microlenses. <https://doi.org/10.1038/NMETH.1339>
- 627 Berens, P., Freeman, J., Deneux, T., Chenkov, N., McColgan, T., Speiser, A., ... Bethge, M. (2017).  
628 Community-based benchmarking improves spike rate inference from two-photon calcium  
629 imaging data. *Community-Based Benchmarking Improves Spike Rate Inference from Two-  
630 Photon Calcium Imaging Data*, 16, 177956. <https://doi.org/10.1101/177956>
- 631 Berezin, M. Y., & Achilefu, S. (2010). Fluorescence lifetime measurements and biological imaging.  
632 *Chemical Reviews*, 110(5), 2641–2684. <https://doi.org/10.1021/cr900343z>
- 633 Beyene, A. G., Delevich, K., Yang, S. J., & Landry, M. P. (2018). New Optical Probes Bring  
634 Dopamine to Light. *Biochemistry*, 57(45), 6379–6381.  
635 <https://doi.org/10.1021/acs.biochem.8b00883>
- 636 Bollmann, J. H., & Engert, F. (2009). Subcellular Topography of Visually Driven Dendritic Activity  
637 in the Vertebrate Visual System. *Neuron*, 61(6), 895–905.  
638 <https://doi.org/10.1016/j.neuron.2009.01.018>
- 639 Bolon, B., & Butt, M. T. (2011). *Fundamental Neuropathology for Pathologists and Toxicologists:  
640 Principles and Techniques*. John Wiley and Sons. <https://doi.org/10.1002/9780470939956>
- 641 Bruinsma, B., Terra, H., de Kloet, S. F., Luchicchi, A., Timmerman, A. J., Rummelink, E., ...  
642 Mansvelder, H. D. (2019). An automated home-cage-based 5-choice serial reaction time task for  
643 rapid assessment of attention and impulsivity in rats. *Psychopharmacology*, 1–12.  
644 <https://doi.org/10.1007/s00213-019-05189-0>
- 645 Campos, P. (2019). Diving into the brain: deep brain imaging techniques in conscious animals.  
646 *Endocrine Abstracts*, 1–35. <https://doi.org/10.1530/endoabs.63.nsa6>
- 647 Cantu, D. A., Wang, B., Gongwer, M. W., He, C. X., Goel, A., Suresh, A., ... Portera-Cailliau, C.  
648 (2020). EZcalcium: Open-Source Toolbox for Analysis of Calcium Imaging Data. *Frontiers in  
649 Neural Circuits*, 14. <https://doi.org/10.3389/fncir.2020.00025>
- 650 Celinskis, D., Friedman, N., Koksharov, M., Murphy, J., Gomez-ramirez, M., Borton, D., ... Moore,  
651 C. (2020). Miniaturized Devices for Bioluminescence Imaging in Freely Behaving Animals.

- 652 *BioRxiv*.
- 653 Chen, T. W., Wardill, T. J., Sun, Y., Pulver, S. R., Renninger, S. L., Baohan, A., ... Kim, D. S.  
654 (2013). Ultrasensitive fluorescent proteins for imaging neuronal activity. *Nature*, 499(7458),  
655 295–300. <https://doi.org/10.1038/nature12354>
- 656 Chen, Y., Lin, Y. C., Kuo, T. W., & Knight, Z. A. (2015). Sensory Detection of Food Rapidly  
657 Modulates Arcuate Feeding Circuits. *Cell*, 160(5), 829–841.  
658 <https://doi.org/10.1016/j.cell.2015.01.033>
- 659 Cobbold, P. H., & Rink, T. J. (1987). Fluorescence and bioluminescence measurement of  
660 cytoplasmic free calcium. *Biochemical Journal*. Biochem J. <https://doi.org/10.1042/bj2480313>
- 661 Da Silva, J. A., Tecuapetla, F., Paixão, V., & Costa, R. M. (2018). Dopamine neuron activity before  
662 action initiation gates and invigorates future movements. *Nature*, 554(7691), 244–248.  
663 <https://doi.org/10.1038/nature25457>
- 664 Dana, H., Sun, Y., Mohar, B., Hulse, B. K., Kerlin, A. M., Hasseman, J. P., ... Kim, D. S. (2019).  
665 High-performance calcium sensors for imaging activity in neuronal populations and  
666 microcompartments. *Nature Methods*, 16(7), 649–657. <https://doi.org/10.1038/s41592-019-0435-6>
- 668 Datta, D., & Arnsten, A. F. T. (2019). Loss of prefrontal cortical higher cognition with uncontrollable  
669 stress: Molecular mechanisms, changes with age, and relevance to treatment. *Brain Sciences*,  
670 9(5), 1–16. <https://doi.org/10.3390/brainsci9050113>
- 671 Daviu, N., Füzesi, T., Rosenegger, D. G., Rasiah, N. P., Sterley, T. L., Peringod, G., & Bains, J. S.  
672 (2020). Paraventricular nucleus CRH neurons encode stress controllability and regulate  
673 defensive behavior selection. *Nature Neuroscience*, 23(3), 398–410.  
674 <https://doi.org/10.1038/s41593-020-0591-0>
- 675 de Groot, A., van den Boom, B. J. G., van Genderen, R. M., Coppens, J., van Veldhuijzen, J., Bos, J.,  
676 ... Hoogland, T. M. (2020). Ninscope, a versatile miniscope for multi-region circuit  
677 investigations. *ELife*, 9, 1–24. <https://doi.org/10.7554/eLife.49987>
- 678 Doetsch, G. S. (2000). Patterns in the brain: Neuronal population coding in the somatosensory  
679 system. *Physiology and Behavior*, 69(1), 187–201. [https://doi.org/10.1016/S0031-9384\(00\)00201-8](https://doi.org/10.1016/S0031-9384(00)00201-8)
- 681 Etter, G., Manseau, F., & Williams, S. (2020). A Probabilistic Framework for Decoding Behavior  
682 From in vivo Calcium Imaging Data. *Frontiers in Neural Circuits*, 14(May), 1–16.  
683 <https://doi.org/10.3389/fncir.2020.00019>
- 684 Farhana, I., Hossain, N., Suzuki, K., Matsuda, T., & Nagai, T. (2019). Genetically Encoded  
685 Fluorescence/Bioluminescence Bimodal Indicators for Ca<sup>2+</sup> Imaging.  
686 <https://doi.org/10.1021/acssensors.9b00531>
- 687 Friedrich, J., Zhou, P., & Paninski, L. (2017). Fast online deconvolution of calcium imaging data.  
688 *PLoS Computational Biology*, 13(3). <https://doi.org/10.1371/journal.pcbi.1005423>

## Methodological comparison between fiber photometry and miniaturized endoscopes

- 689 Ghosh, K. K., Burns, L. D., Cocker, E. D., Nimmerjahn, A., Ziv, Y., Gamal, A. El, & Schnitzer, M.  
690 J. (2011). Miniaturized integration of a fluorescence microscope. *Articles Nsture Methods*,  
691 8(10). <https://doi.org/10.1038/Nmeth.1694>
- 692 Giovannucci, A., Friedrich, J., Gunn, P., Kalfon, J., Brown, B. L., Koay, S. A., ... Pnevmatikakis, E.  
693 A. (2019). CaImAn an open source tool for scalable calcium imaging data analysis. *ELife*, 8.  
694 <https://doi.org/10.7554/eLife.38173>
- 695 Girven, K. S., & Sparta, D. R. (2017). Probing Deep Brain Circuitry: New Advances in in Vivo  
696 Calcium Measurement Strategies. *ACS Chemical Neuroscience*.  
697 <https://doi.org/10.1021/acschemneuro.6b00307>
- 698 Glas, A., Hübener, M., Bonhoeffer, T., & Goltstein, P. M. (2019). Benchmarking miniaturized  
699 microscopy against two-photon calcium imaging using single-cell orientation tuning in mouse  
700 visual cortex. *PLoS ONE*, 14(4). <https://doi.org/10.1371/journal.pone.0214954>
- 701 Gonzalez, W., Zhang, H., Harutyunyan, A., & Lois, C. (2019). Persistence of neuronal  
702 representations through time and damage in the hippocampus. *Science*, 559104.  
703 <https://doi.org/10.1101/559104>
- 704 Grienberger, C., & Konnerth, A. (2012, March 8). Imaging Calcium in Neurons. *Neuron*. Neuron.  
705 <https://doi.org/10.1016/j.neuron.2012.02.011>
- 706 Gunaydin, L. A., Grosenick, L., Finkelstein, J. C., Kauvar, I. V., Fenno, L. E., Adhikari, A., ...  
707 Deisseroth, K. (2014). Natural neural projection dynamics underlying social behavior. *Cell*,  
708 157(7), 1535–1551. <https://doi.org/10.1016/j.cell.2014.05.017>
- 709 Hamel, E. J. O., Grewe, B. F., Parker, J. G., & Schnitzer, M. J. (2015, April 8). Cellular level brain  
710 imaging in behaving mammals: An engineering approach. *Neuron*. Cell Press.  
711 <https://doi.org/10.1016/j.neuron.2015.03.055>
- 712 Helmchen, F. (2009). Two-Photon Functional Imaging of Neuronal Activity (pp. 37–58). CRC  
713 Press/Taylor & Francis. <https://doi.org/10.1201/9781420076851.ch2>
- 714 Helmchen, F., Fee, M. S., Tank, D. W., & Denk, W. (2001). A miniature head-mounted two-photon  
715 microscope: High-resolution brain imaging in freely moving animals. *Neuron*, 31(6), 903–912.  
716 [https://doi.org/10.1016/S0896-6273\(01\)00421-4](https://doi.org/10.1016/S0896-6273(01)00421-4)
- 717 Herculano-Houzel, S., Mota, B., & Lent, R. (2006). *Cellular scaling rules for rodent brains*.  
718 Retrieved from [www.pnas.org/cgi/doi/10.1073/pnas.0604911103](http://www.pnas.org/cgi/doi/10.1073/pnas.0604911103)
- 719 Heidbreder, C. A., & Groenewegen, H. J. (2003). The medial prefrontal cortex in the rat: Evidence  
720 for a dorso-ventral distinction based upon functional and anatomical characteristics.  
721 *Neuroscience and Biobehavioral Reviews*, 27(6), 555–579.  
722 <https://doi.org/10.1016/j.neubiorev.2003.09.003>
- 723 Hohlbaum, K., Bert, B., Dietze, S., Palme, R., Fink, H., & Thöne-Reineke, C. (2017). Severity  
724 classification of repeated isoflurane anesthesia in C57BL/6JRj mice - Assessing the degree of  
725 distress. *PLoS ONE*, 12(6). <https://doi.org/10.1371/journal.pone.0179588>

- 726 Inoue, M., Takeuchi, A., Manita, S., Horigane, S. ichiro, Sakamoto, M., Kawakami, R., ... Bito, H.  
 727 (2019). Rational Engineering of XCaMPs, a Multicolor GECI Suite for In Vivo Imaging of  
 728 Complex Brain Circuit Dynamics. *Cell*, *177*(5), 1346-1360.e24.  
 729 <https://doi.org/10.1016/j.cell.2019.04.007>
- 730 Ivashkina, O. I., Gruzdeva, A. M., Roshchina, M. A., Toropova, K. A., & Anokhin, K. V. (2019). Ex  
 731 vivo and in vivo imaging of mouse parietal association cortex activity in episodes of cued fear  
 732 memory formation and retrieval. *BioRxiv*, 863589. <https://doi.org/10.1101/863589>
- 733 Josselyn, S. A., & Tonegawa, S. (2020). Memory engrams: Recalling the past and imagining the  
 734 future. *Science*, *367*(6473). <https://doi.org/10.1126/science.aaw4325>
- 735 Jun, J. J., Steinmetz, N. A., Siegle, J. H., Denman, D. J., Bauza, M., Barbarits, B., ... Harris, T. D.  
 736 (2017). Fully integrated silicon probes for high-density recording of neural activity. *Nature*,  
 737 *551*(7679), 232–236. <https://doi.org/10.1038/nature24636>
- 738 Khiarak, M. N., Martianova, E., Bories, C., Martel, S., Proulx, C. D., De Koninck, Y., & Gosselin, B.  
 739 (2018). A Wireless Fiber Photometry System Based on a High-Precision CMOS Biosensor with  
 740 Embedded Continuous-Time  $\Sigma \Delta$  Modulation. *IEEE Transactions on Biomedical Circuits and*  
 741 *Systems*, *12*(3), 495–509. <https://doi.org/10.1109/TBCAS.2018.2817200>
- 742 Kim, C. K., Yang, S. J., Pichamoorthy, N., Young, N. P., Kauvar, I., Jennings, J. H., ... Deisseroth,  
 743 K. (2016). simultaneous fast measurement of circuit dynamics at multiple sites across the  
 744 mammalian brain, *13*(4), 325. <https://doi.org/10.1038/Nmeth.3770>
- 745 Kitamura, T., Ogawa, S. K., Roy, D. S., Okuyama, T., Morrissey, M. D., Smith, L. M., ... Tonegawa,  
 746 S. (2017). Engrams and circuits crucial for systems consolidation of a memory. *Science*,  
 747 *356*(6333), 73–78. <https://doi.org/10.1126/science.aam6808>
- 748 Krohn, T. C., Sørensen, D. B., Ottesen, J. L., & Hansen, A. K. (2006). The effects of individual  
 749 housing on mice and rats: A review. Retrieved May 29, 2020, from  
 750 <https://psycnet.apa.org/record/2008-10455-001>
- 751 Kupferschmidt, D. A., Juczewski, K., Cui, G., Johnson, K. A., & Lovinger, D. M. (2017). Parallel,  
 752 but Dissociable, Processing in Discrete Corticostriatal Inputs Encodes Skill Learning. *Neuron*,  
 753 *96*(2), 476-489.e5. <https://doi.org/10.1016/j.neuron.2017.09.040>
- 754 Lecca, S., Namboodiri, V. M. K., Restivo, L., Gervasi, N., Pillolla, G., Stuber, G. D., & Mameli, M.  
 755 (2020). Heterogeneous Habenular Neuronal Ensembles during Selection of Defensive  
 756 Behaviors. *Cell Reports*, *31*(10). <https://doi.org/10.1016/j.celrep.2020.107752>
- 757 Li, L., Tang, Y., Sun, L., Rahman, K., Huang, K., Xu, W., ... Cao, G. (2017). In vivo fiber  
 758 photometry of neural activity in response to optogenetically manipulated inputs in freely moving  
 759 mice. *Journal of Innovative Optical Health Sciences*, *10*(5).  
 760 <https://doi.org/10.1142/S1793545817430015>
- 761 Li, Y., Liu, Z., Guo, Q., & Luo, M. (2019). Long-term Fiber Photometry for Neuroscience Studies.  
 762 *Neuroscience Bulletin*, *35*(3), 425–433. <https://doi.org/10.1007/s12264-019-00379-4>
- 763 Liang, B., Zhang, L., Barbera, G., Chen, R., Li, Y., & Lin, D.-T. (2018). Distinct and Dynamic ON



## Methodological comparison between fiber photometry and miniaturized endoscopes

- 764 and OFF Neural Ensembles in the Prefrontal Cortex Code Social Exploration. *Neuron*, *100*, 700-  
765 714.e9. <https://doi.org/10.1016/j.neuron.2018.08.043>
- 766 Lonsdorf, T. B., Menz, M. M., Andreatta, M., Fullana, M. A., Golkar, A., Haaker, J., ... Merz, C. J.  
767 (2017). Don't fear 'fear conditioning': Methodological considerations for the design and  
768 analysis of studies on human fear acquisition, extinction, and return of fear. *Neuroscience and*  
769 *Biobehavioral Reviews*, *77*, 247–285. <https://doi.org/10.1016/j.neubiorev.2017.02.026>
- 770 Lopes, G., Bonacchi, N., Frazão, J., Neto, J. P., Atallah, B. V., Soares, S., ... Kampff, A. R. (2015).  
771 Bonsai: an event-based framework for processing and controlling data streams. *Frontiers in*  
772 *Neuroinformatics*, *9*(APR), 7. <https://doi.org/10.3389/fninf.2015.00007>
- 773 Lu, J., Li, C., Singh-Alvarado, J., Zhou, C., Frö, F., Mooney, R., & Wang, F. (2018). MIN1PIPE: A  
774 Miniscope 1-Photon-Based Calcium Imaging Signal Extraction Pipeline. *Cell Reports*, *23*,  
775 3673–3684. <https://doi.org/10.1016/j.celrep.2018.05.062>
- 776 Lu, L., Gutruf, P., Xia, L., Bhatti, D. L., Wang, X., Vazquez-Guardado, A., ... Rogers, J. A. (2018).  
777 Wireless optoelectronic photometers for monitoring neuronal dynamics in the deep brain.  
778 *Proceedings of the National Academy of Sciences of the United States of America*, *115*(7),  
779 E1374–E1383. <https://doi.org/10.1073/pnas.1718721115>
- 780 Ma, Q., Ye, L., Liu, H., Shi, Y., & Zhou, N. (2017, May 4). An overview of Ca<sup>2+</sup> mobilization  
781 assays in GPCR drug discovery. *Expert Opinion on Drug Discovery*. Taylor and Francis Ltd.  
782 <https://doi.org/10.1080/17460441.2017.1303473>
- 783 Manouze, H., Ghestem, A., Poillerat, V., Bennis, M., Ba-M'hamed, S., Benoliel, J. J., ... Bernard, C.  
784 (2019). Effects of single cage housing on stress, cognitive, and seizure parameters in the rat and  
785 mouse pilocarpine models of epilepsy. *ENeuro*, *6*(4). [https://doi.org/10.1523/ENEURO.0179-](https://doi.org/10.1523/ENEURO.0179-18.2019)  
786 18.2019
- 787 Marvin, J. S., Borghuis, B. G., Tian, L., Cichon, J., Harnett, M. T., Akerboom, J., ... Looger, L. L.  
788 (2013). An optimized fluorescent probe for visualizing glutamate neurotransmission. *Nature*  
789 *Methods*, *10*(2), 162–170. <https://doi.org/10.1038/nmeth.2333>
- 790 Mathis, A., Mamidanna, P., Cury, K. M., Abe, T., Murthy, V. N., Mathis, M. W., & Bethge, M.  
791 (2018). DeepLabCut: markerless pose estimation of user-defined body parts with deep learning.  
792 *Nature Neuroscience*, *21*(9), 1281–1289. <https://doi.org/10.1038/s41593-018-0209-y>
- 793 Matos, M. R., Visser, E., Kramvis, I., van der Loo, R. J., Gebuis, T., Zalm, R., ... van den Oever, M.  
794 C. (2019). Memory strength gates the involvement of a CREB-dependent cortical fear engram in  
795 remote memory. *Nature Communications*, *10*(1). <https://doi.org/10.1038/s41467-019-10266-1>
- 796 Musall, S., Kaufman, M. T., Juavinett, A. L., Gluf, S., & Churchland, A. K. (2019). Single-trial  
797 neural dynamics are dominated by richly varied movements. *Nature Neuroscience*, *22*(10),  
798 1677–1686. <https://doi.org/10.1038/s41593-019-0502-4>
- 799 Nakai, J., Ohkura, M., & Imoto, K. (2001). A high signal-to-noise ca<sup>2+</sup> probe composed of a single  
800 green fluorescent protein. *Nature Biotechnology*, *19*(2), 137–141. <https://doi.org/10.1038/84397>
- 801 Nicolelis, M. (2011). *Beyond boundaries : the new neuroscience of connecting brains with machines-*

- 802        -and how it will change our lives (1st ed.). New York: Times Books/Henry Holt and Co.
- 803    Nicolelis, M. A. L., Ghazanfar, A. A., Stambaugh, C. R., Oliveira, L. M. O., Laubach, M., Chapin, J.  
804        K., ... Kaas, J. H. (1998). Simultaneous encoding of tactile information by three primate cortical  
805        areas. *Nature Neuroscience*, *1*(7), 621–630. <https://doi.org/10.1038/2855>
- 806    Noorshams, O., Boyd, J. D., & Murphy, T. H. (2017). Automating mouse weighing in group  
807        homecages with Raspberry Pi micro-computers. *Journal of Neuroscience Methods*, *285*, 1–5.  
808        <https://doi.org/10.1016/j.jneumeth.2017.05.002>
- 809    Oh, J., Lee, C., & Kaang, B. K. (2019, July 1). Imaging and analysis of genetically encoded calcium  
810        indicators linking neural circuits and behaviors. *Korean Journal of Physiology and*  
811        *Pharmacology*. Korean Physiological Soc. and Korean Soc. of Pharmacology.  
812        <https://doi.org/10.4196/kjpp.2019.23.4.237>
- 813    Ouzounov, D. G., Wang, T., Wang, M., Feng, D. D., Horton, N. G., Cruz-Hernández, J. C., ... Xu, C.  
814        (2017). In vivo three-photon imaging of activity of Gcamp6-labeled neurons deep in intact  
815        mouse brain. *Nature Methods*, *14*(4), 388–390. <https://doi.org/10.1038/nmeth.4183>
- 816    Owen, S. F., & Kreitzer, A. C. (2019). An open-source control system for in vivo fluorescence  
817        measurements from deep-brain structures. *Journal of Neuroscience Methods*, *311*, 170–177.  
818        <https://doi.org/10.1016/j.jneumeth.2018.10.022>
- 819    Parker, P. R. L., Brown, M. A., Smear, M. C., & Niell, C. M. (2020). Movement-Related Signals in  
820        Sensory Areas: Roles in Natural Behavior. *Trends in Neurosciences*, 1–15.  
821        <https://doi.org/10.1016/j.tins.2020.05.005>
- 822    Pisanello, M., Pisano, F., Hyun, M., Maglie, E., Balena, A., De Vittorio, M., ... Pisanello, F. (2018).  
823        Analytical and empirical measurement of fiber photometry signal volume in brain tissue, *i*, 1–  
824        41. Retrieved from <http://arxiv.org/abs/1807.03023>
- 825    Pisano, F., Pisanello, M., Lee, S. J., Lee, J., Maglie, E., Balena, A., ... Pisanello, F. (2019). Depth-  
826        resolved fiber photometry with a single tapered optical fiber implant. *Nature Methods*, *16*(11),  
827        1185–1192. <https://doi.org/10.1038/s41592-019-0581-x>
- 828    Pnevmatikakis, E. A. (2019). Analysis pipelines for calcium imaging data. *Current Opinion in*  
829        *Neurobiology*, *55*, 15–21. <https://doi.org/10.1016/j.conb.2018.11.004>
- 830    Pnevmatikakis, E. A., & Giovannucci, A. (2017). NoRMCorre: An online algorithm for piecewise  
831        rigid motion correction of calcium imaging data. *Journal of Neuroscience Methods*, *291*, 83–94.  
832        <https://doi.org/10.1016/j.jneumeth.2017.07.031>
- 833    Powell, N. J., & Redish, A. D. (2016). Representational changes of latent strategies in rat medial  
834        prefrontal cortex precede changes in behaviour. *Nature Communications*, *7*.  
835        <https://doi.org/10.1038/ncomms12830>
- 836    Resendez, S. L., Jennings, J. H., Ung, R. L., Namboodiri, V. M. K., Zhou, Z. C., Otis, J. M., ...  
837        Stuber, G. D. (2016). Visualization of cortical, subcortical and deep brain neural circuit  
838        dynamics during naturalistic mammalian behavior with head-mounted microscopes and  
839        chronically implanted lenses. *Nature Protocols*, *11*(3), 566–597.

## Methodological comparison between fiber photometry and miniaturized endoscopes

- 840 <https://doi.org/10.1038/nprot.2016.021>
- 841 Resendez, S. L., & Stuber, G. D. (2015). In Vivo Calcium Imaging to Illuminate Neurocircuit  
842 Activity Dynamics Underlying Naturalistic Behavior. *Neuropsychopharmacology* 2015 40:1,  
843 40(1), 238–239. <https://doi.org/10.1038/npp.2014.206>
- 844 Ross, W. N. (1989). Changes in intracellular calcium during neuron activity. *Annu. Rev. Physiol.*,  
845 (51), 491–506. Retrieved from [www.annualreviews.org](http://www.annualreviews.org)
- 846 Sabatini, B. L. (2019). The impact of reporter kinetics on the interpretation of data gathered with  
847 fluorescent reporters. *BioRxiv*. <https://doi.org/10.1017/CBO9781107415324.004>
- 848 Scanziani, M., & Häusser, M. (2009, October 15). Electrophysiology in the age of light. *Nature*.  
849 Nature Publishing Group. <https://doi.org/10.1038/nature08540>
- 850 Seo, C., Guru, A., Jin, M., Ito, B., Sleezer, B. J., Ho, Y.-Y., ... Warden, M. R. (2019). *Intense threat*  
851 *switches dorsal raphe serotonin neurons to a paradoxical operational mode* Downloaded from.  
852 *Science* (Vol. 363). Retrieved from <http://science.sciencemag.org/>
- 853 Sheintuch, L., Rubin, A., Brande-Eilat, N., Geva, N., Sadeh, N., Pinchasof, O., & Ziv, Y. (2017).  
854 Tracking the Same Neurons across Multiple Days in Ca<sup>2+</sup> Imaging Data. *Cell Reports*, 21(4),  
855 1102–1115. <https://doi.org/10.1016/j.celrep.2017.10.013>
- 856 Shuman, T., Aharoni, D., Cai, D. J., Lee, C. R., Chavlis, S., Page-Harley, L., ... Golshani, P. (2020).  
857 Breakdown of spatial coding and interneuron synchronization in epileptic mice. *Nature*  
858 *Neuroscience*, 23(2), 229–238. <https://doi.org/10.1038/s41593-019-0559-0>
- 859 Silva, A. J. (2017). Miniaturized two-photon microscope: Seeing clearer and deeper into the brain.  
860 *Light: Science and Applications*, 6(8). <https://doi.org/10.1038/lsa.2017.104>
- 861 Simone, K., Füzesi, T., Rosenegger, D., Bains, J., & Murari, K. (2018). Open-source, cost-effective  
862 system for low-light in vivo fiber photometry. *NeuroPhotonics*, 5(02), 1.  
863 <https://doi.org/10.1117/1.nph.5.2.025006>
- 864 Song, C., Barnes, S., & Knöpfel, T. (2017). Mammalian cortical voltage imaging using genetically  
865 encoded voltage indicators: a review honoring professor Amiram Grinvald. *NeuroPhotonics*,  
866 4(3), 031214. <https://doi.org/10.1117/1.nph.4.3.031214>
- 867 Steinmetz, N. A., Buetfering, C., Lecoq, J., Lee, C. R., Peters, A. J., Jacobs, E. A. K., ... Harris, K.  
868 D. (2017). Aberrant cortical activity in multiple GCaMP6-expressing transgenic mouse lines.  
869 *ENeuro*, 4(5). <https://doi.org/10.1523/ENEURO.0207-17.2017>
- 870 Sych, Y., Chernysheva, M., Sumanovski, L. T., & Helmchen, F. (2019). High-density multi-fiber  
871 photometry for studying large-scale brain circuit dynamics. *Nature Methods*, 16(6), 553–560.  
872 <https://doi.org/10.1038/s41592-019-0400-4>
- 873 Tegtmeier, J., Brosch, M., Janitzky, K., Heinze, H.-J., Ohl, F. W., & Lippert, M. T. (2018). CAVE:  
874 An Open-Source Tool for Combined Analysis of Head-Mounted Calcium Imaging and Behavior  
875 in MATLAB. *Frontiers in Neuroscience*, 12, 958. <https://doi.org/10.3389/fnins.2018.00958>

- 876 Tian, L., Hires, S. A., Mao, T., Huber, D., Chiappe, M. E., Chalasani, S. H., ... Looger, L. L. (2009).  
877 Imaging neural activity in worms, flies and mice with improved GCaMP calcium indicators.  
878 *Nature Methods*, 6(12), 875–881. <https://doi.org/10.1038/nmeth.1398>
- 879 Wu, L., Zhao, H., Weng, H., & Ma, D. (2019, April 19). Lasting effects of general anesthetics on the  
880 brain in the young and elderly: “mixed picture” of neurotoxicity, neuroprotection and cognitive  
881 impairment. *Journal of Anesthesia*. Springer Tokyo. [https://doi.org/10.1007/s00540-019-02623-](https://doi.org/10.1007/s00540-019-02623-7)  
882 7
- 883 Yang, L., Zhao, Y., Wang, Y., Liu, L., Zhang, X., Li, B., & Cui, R. (2015). The Effects of  
884 Psychological Stress on Depression. *Current Neuropharmacology*, 13(4), 494–504.  
885 <https://doi.org/10.2174/1570159X1304150831150507>
- 886 Yang, Y., Liu, N., He, Y., Liu, Y., Ge, L., Zou, L., ... Liu, X. (2018). Improved calcium sensor  
887 GCaMP-X overcomes the calcium channel perturbations induced by the calmodulin in GCaMP.  
888 *Nature Communications*, 9(1). <https://doi.org/10.1038/s41467-018-03719-6>
- 889 Zalocusky, K. A., Ramakrishnan, C., Lerner, T. N., Davidson, T. J., Knutson, B., & Deisseroth, K.  
890 (2016). Nucleus accumbens D2R cells signal prior outcomes and control risky decision-making.  
891 *Nature*, 531. <https://doi.org/10.1038/nature17400>
- 892 Zhang, L., Liang, B., Barbera, G., Hawes, S., Zhang, Y., Stump, K., ... Lin, D. T. (2019). Miniscope  
893 GRIN Lens System for Calcium Imaging of Neuronal Activity from Deep Brain Structures in  
894 Behaving Animals. *Current Protocols in Neuroscience*, 86(1), 1–21.  
895 <https://doi.org/10.1002/cpns.56>
- 896 Zhou, P., Resendez, S. L., Rodriguez-Romaguera, J., Jimenez, J. C., Neufeld, S. Q., Giovannucci, A.,  
897 ... Paninski, L. (2018). Efficient and accurate extraction of in vivo calcium signals from  
898 microendoscopic video data. *ELife*, 7. <https://doi.org/10.7554/eLife.28728>
- 899 Zong, W., Wu, R., Li, M., Hu, Y., Li, Y., Li, J., ... Cheng, H. (2017). Fast high-resolution miniature  
900 two-photon microscopy for brain imaging in freely behaving mice. *Nature Methods*, 14(7), 713–  
901 719. <https://doi.org/10.1038/nmeth.4305>
- 902 Zucker, R. S. (1999). Calcium- and activity-dependent synaptic plasticity. *Current Opinion in*  
903 *Neurobiology*, 9(3), 305–313. [https://doi.org/10.1016/S0959-4388\(99\)80045-2](https://doi.org/10.1016/S0959-4388(99)80045-2)